# A cooled telescope for measurements of the Near Infrared Cosmological Background at balloon altitude (TRIP Experiment) (*)

M. R. Attolini ([1]), A. Boscaleri ([2]), A. Brighenti ([1]), P. Cazzola ([1]), P. Calzolari ([1])
S. Cortiglioni ([1]), G. Giovannini ([1]), M. Malaspina ([1]), N. Mandolesi ([1])
G. Morigi ([1]), E. Palazzi ([1]) and G. Ventura ([1])

([1]) *Istituto TESRE / CNR - Via Gobetti 101, 40129 Bologna, Italy*
([2]) *IROE / CNR - Via Panciatichi 64, 50127 Firenze, Italy*

(ricevuto il 5 Dicembre 1996; approvato il 25 Febbraio 1997)

**Summary.** — A cooled telescope has been designed and prepared for measurements of both local and cosmological Near InfraRed Backgrounds in the waveband 1–5 $\mu$m at balloon altitude (40 km). The detection system consists of a linear array with 32 InSb pixels placed in the focal plane of the telescope, cryogenically cooled and thermally controlled. A short description is given of the main characteristics of the instrument and of the expected performances. The experiment, repeatedly tested in laboratory, flew in the 1995 summer from Palestine (Texas, USA).

PACS 94.40 – Cosmic rays.
PACS 01.30.Cc – Conference proceedings.

## 1. – Introduction

The origin and source of the Near Infrared Cosmological Background (NIRB) is of great interest to cosmology as it is likely to originate at a redshift of $5 < z < 1000$. Physical processes taking place at that epoch, expecially galaxy formation, remain poorly understood. A large theoretical effort has been devoted to this subject, however an adequate number of observations to probe this epoch has not followed. The lack of observations is mainly due to the fact that it is practically impossible to perform them from ground due to strong atmospheric thermal and line emission. The total NIRB intensity flux is a combination of the extragalactic background and some local backgrounds such as zodiacal light (ZL), interplanetary dust (IPD), integrated star light

(*) Paper presented at the VII Cosmic Physics National Conference, Rimini, October 26-28, 1994.

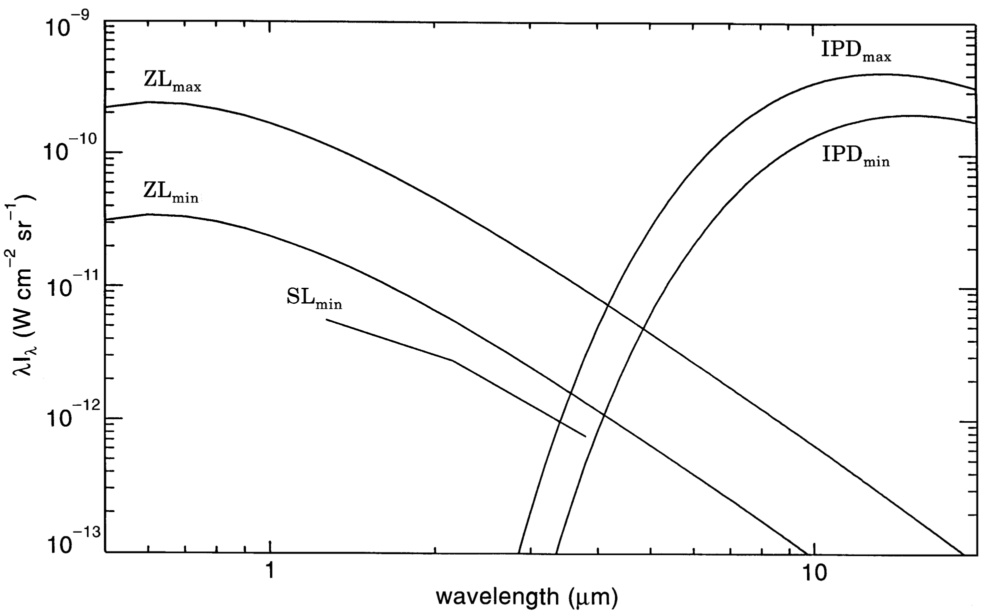


Fig. 1. – The expected IR local background emissions.

(SL), atmospheric emission and OH emission. Hence it is necessary to distinguish between each different component to detect the cosmological extragalactic background.

Observations in the waveband 1–5 $\mu$m are easier for two reasons: first of all, the contribution by zodiacal light and star light decreases rapidly as the wavelength increases, while the cosmological background probably has a flat spectrum due to the redshift; second, the contribution of nearby galaxies, unlike that of the NIRB which originates at high redshift, falls at optical wavelengths. The scenario which appears to observers is represented in fig. 1. Estimates for the local background are available from the models developed by different authors on the basis of existing data [1-5]. The detection of a NIRB was first reported by Matsumoto *et al.* from his rocket experiments [6]. The measured intensity is $I = 10^5$ Jy sr$^{-1}$ at $\lambda = 2.2\,\mu$m and it is consistent with a 1500 K black body diluted by a factor $10^{-11}$.

This intensity value exceeds by a sizeable factor the predictions based on source counts and on current galaxy evolution models.

At the moment further observations are needed to confirm the existence of an excess in the diffuse NIRB over the local emission.

To perform the measurement the use of satellite-, rocket- or balloon-borne instruments is required. The first solution, although the best, would imply high costs and a long time of realization. Due to the short life of a rocket flight, the second solution implies short observing time and a poor sky coverage, with the additional problem of pollution from the engine exhaust gas which is hard to evaluate. Stratospheric balloons, on the other hand, permit long flights with fair sky coverage at a lower manufacturing cost, the only problem being the residual atmosphere at about 40 km altitude.

We have chosen a balloon-borne experiment, because we think that, in order to find a compromise between the costs and the scientific aims, it is the most suitable solution among the three mentioned above. The TRIP balloon successfully flew in June 1995.

## 2. – Payload configuration

The gondola is a prism of about 1.7 m $\times$ 2.0 m $\times$ 1.0 m with a weight of about 850 kg. The central supporting column is fixed to the azimuth-pointing system and then to the balloon flight chain. The inner volume of the gondola is divided into three parts: one (gondola north) is reserved for the IR telescope and the zenith system, the opposite side (gondola south) is occupied by the electronics and the batteries, the central part is reserved for the LHe dewar, the pressure control system and the telemetry package.

## 3. – The optics and the filter system

To observe the IR background in the wavelength range 1–5 $\mu$m at about 40 km altitude, one has to use a cooled apparatus to minimize the thermal emission from the mirrors and the telescope mounting. This strongly limits the size of the primary mirror since a large diameter implies a big cryostat not allowed for a balloon experiment. Background observations need in general a quite large field of view to permit large sky coverage and a small angular scale at the focal plane to discriminate against point-like sources. These considerations, together with the constraints imposed by detector size and geometry, led to design a double Cassegrain optics system with an $F/2$ focal ratio. Figure 2 shows the cross-sectional view of the telescope. The detector optics assembly, including the filter wheel carrying six filters, is placed inside the cryostat and operates at temperatures in the range $45\ \mathrm{K} < T < 55\ \mathrm{K}$.

## 4. – The cryogenic apparatus

The need of a cryogenic apparatus is mainly dictated by two reasons:

– The InSb detector noise performance improves at low temperatures ($\approx 50$ K); also the exposure time needed to reach the detector saturation lengthens as the temperature is lowered.

– The materials surrounding the detector (detector housing, detector assembly, optics and so on) give a contribution to the overall system noise due to their thermal emission which tends to mask the IR background to be measured. This «instrument noise component» is almost negligible if the surfaces which are in the field of view of the detector are cooled below 120 K.

In the storage dewar, liquid He is boiled by controlling the current through four heating elements, so that an increase of the internal pressure forces the He flow into the transfer line. Figure 3 schematically shows the system used to control and stabilize the temperature during the flight [7].

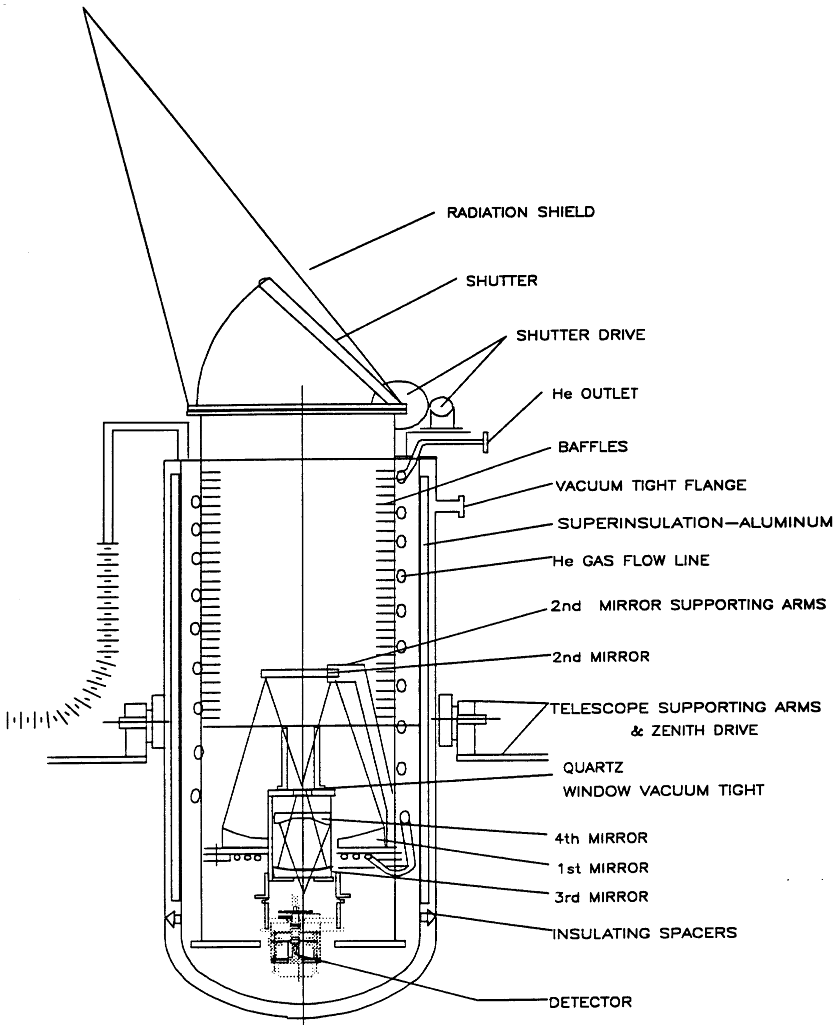


Fig. 2. – Cross-sectional view of the telescope.

## 5. – The detector and associated electronics

The focal plane detector is a linear array consisting of 32 InSb integrating photodiodes on which the IR signal is detected and stored during the exposition period. A shift register multiplexes the detectors onto a single output line connected to a JFET preamplifier acting as output buffer while a MOSFET switch is used for resetting and biasing the array. A temperature sensor gives the operating temperature of the detector [8, 9].

The main noise components which limit the detector response in the present application are the *dark current* (which adds to the signal charge stored in the detector during the exposition; when long integration times are used to detect weak IR signals, the detector is «*background limited*» by this noise contribution) and kTC *reset noise*

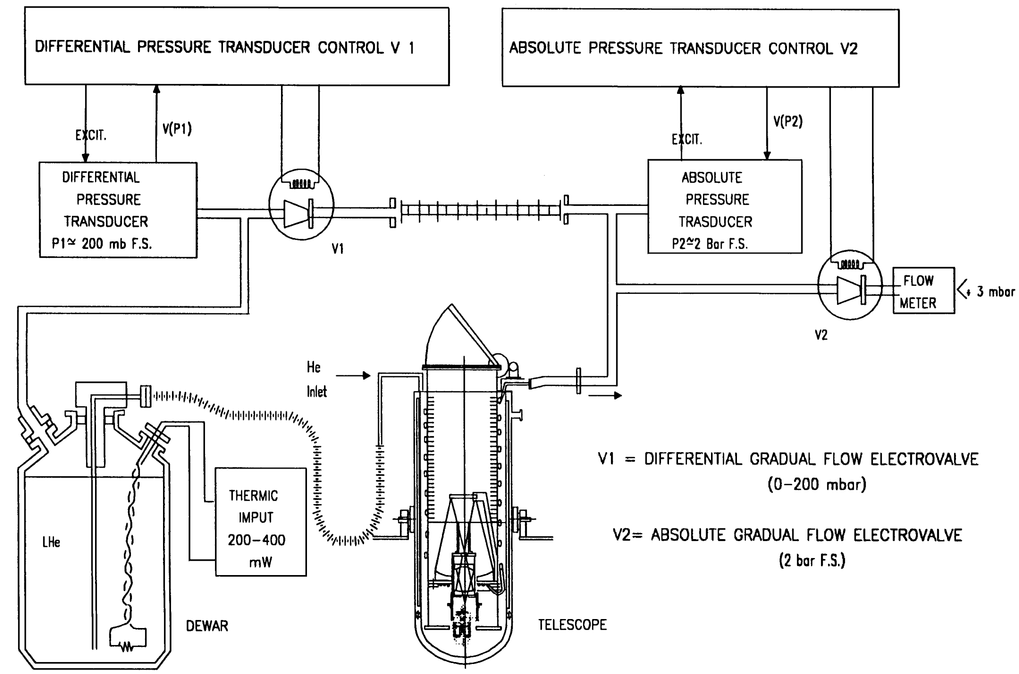


Fig. 3. – Cryogenics control system.

(which sets a limit on the minimum detectable signal when short exposure times are used in the presence of high IR backgrounds).

The detector electronics (NIME-100) performs the following functions:

– Timing generation for the detector clocks.

– Power supplies to bias the detector chip.

– Amplification of the detector signal.

– Compensation for the temperature drifts of the video line (detector signal) and stabilization of the detector temperature at $50 \pm 0.1$ K.

The detector electronics receives the ReadOut command from the on-board CPU and sends the amplified detector signal to the A-to-D electronics: the signal is here converted to 16-bit data words and sent to the CPU for data transmission. The exposure time is set by the time between two successive readout commands. Since the signal accumulated in each pixel is given by the difference between the *signal* portion of the video line and the *zero* voltage level following the application of the reset pulse, each pixel data is represented by two 16-bit words which are separately transmitted to ground. The A/D converter is periodically recalibrated during the flight.

## 6. – The azimuthal stabilization system

Since the infrared telescope elevation is independently controlled by the main experiment CPU, the pointing system can simply be referred to as a *single axis* stabilization. This implies that the system is able to drive the platform around the gravity vector only.

Like many pointing systems it uses a *relatively* cheap position sensor, *i.e.* a magnetometer, mounted on a motorized platform: this permits the change of *azimuth* observation direction either by remote commands or by on-board software.

The system has been designed to stabilize payloads with weight up to 2500 kg with a safety factor of 10 g, is fully under digital control and oversees both the gondola movements and the magnetometer platform changes [10]. The overall system pointing accuracy was measured during integration tests to be of the order of $\pm 15$ arcmin. Furthermore, the aspect field of view will be controlled in quas-real time by using a CCD camera mounted on-axis with the IR telescope.

## 7. – The flight control system (FCS)

The FCS is built around two CPUs, the *Main CPU* (a VME commercial board from Dynatem based on a 68030 CMOS processor) and the *Detector CPU* (also a VME Dynatem board based on a 68000 CMOS processor). The VME crate also includes some boards specifically designed and built to perform dedicated functions [11].

## 8. – The ground program

The ground software equipment runs on several different CPUs. The *REAL-TIME CPU* (Motorola VME133 at 16 MHz) is the input and output interface with the flying experiment. Through a synchronous serial ISR controlled flow, it acquires the formats

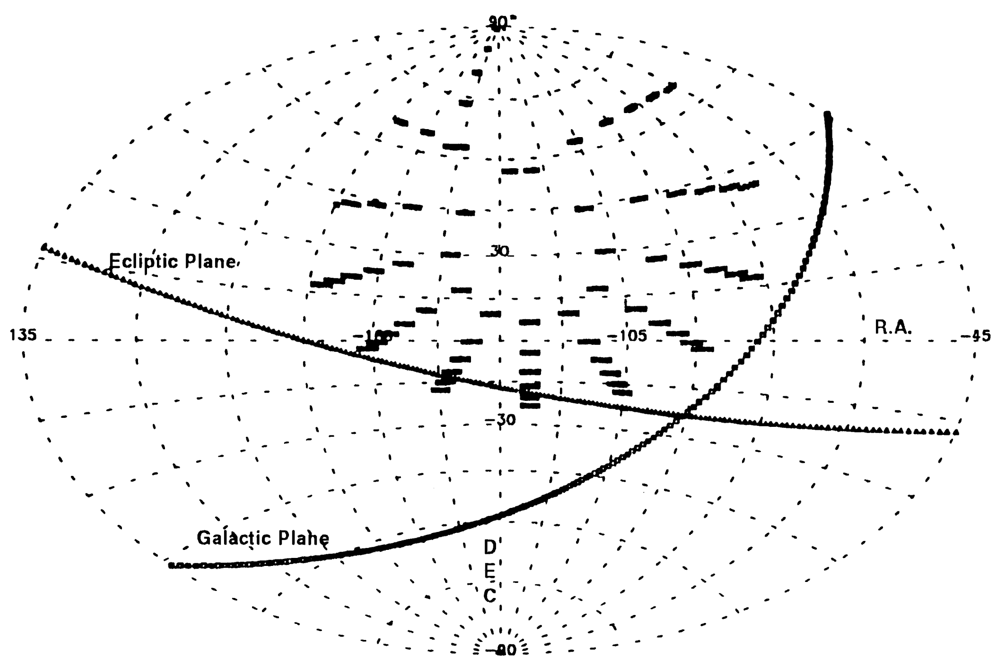


Fig. 4. – The expected sky coverage for a single run of measurements. This example refers to a launch on May 30, 1995 at 20:00 (LT), from the NSBF base of Palestine (Texas, USA).

and makes them available on the dual-ported memory. Furthermore, it provides the parallel strobed output for the telecommands which are to be sent to the experiment. Several PCs can be connected via LAN as clients. There is a general-purpose software, running under Windows 3.1, which performs data analysis and controls graphical display, dialog-boxes, etc. This software has been developed using C + + and allows the operator to have complete control of the whole experiment in real-time [12].

## 9. – Observational techniques and calibrations

The observations consist of a series of scans in azimuth and zenith with all filters (see fig. 4 for a typical observation run). At the end of each zenith scan (five positions) and before changing the filter, a calibration routine for testing and monitoring the system stability will take place in the observing program. This routine consists essentially of an ON / OFF switching sequence of internal lamps and dark current measurements.

Considering the characteristics of both the optics and the detector and the capability of the pointing system to look for point-like sources, absolute in-flight calibrations will require a consistent lot of time and a dedicated routine. Depending on the flight site, date and time, a list of observable known sources will be prepared with related sky positions, fluxes and proper integration times. After a calibration source is selected, the calibration routine will perform a sort of raster scan around the expected source positon. The very thin detector field of view $(1.4' \times 49')$ forces us to this procedure, even if very time expensive. After the recognition of the first source it will be possible also to set up the pointing system offsets, thus making the acquisition of next calibration sources easier. Due to its complexity, one or possibly two absolute calibration procedures are planned at the start of each flight, before running the observing program.

Precise on-ground calibrations are difficult because it is impossible to open the lid of the cryostat when the telescope is cold, so it is not possible to illuminate the whole primary mirror from the outside. For on-ground calibrations we use the internal wall of the lid which was black painted so as to behave as a black body with emissivity of about 97% in the $K$ band. The non-uniformity of the temperature on the surface introduces an error that we estimate to be not more than 10%.

## REFERENCES


[1] Murdock T. L. and Price S. D., *Astron. J.*, **90** (1985) 375.
[2] Bahacall J. N. and Soneira R. M., *Astrophys. J. Suppl.*, **44** (1980) 73.
[3] Mamon A. G. and Soneira R. M., *Astrophys. J.*, **255** (1982) 181.
[4] Franceschini A. *et al.*, *Astron. Astrophys. J. Suppl.*, **89** (1991) 285.
[5] MacClatchey R. A. *et al.*, AFCRL-TR-55-213 (1972).
[6] Matsumoto T. *et al.*, *Astrophys. J.*, **332** (1988) 575.
[7] Cortiglioni S. *et al.*, TESRE / CNR Int. Rep. N. 119 (1986).
[8] Davies R. M. and Nyblack C. A., *Proc. SPIE*, **627** (1986) 438.
[9] Nyblack C. A., *Proceedings of the 28th Midwest Symposium on Circuits and Systems Conference, Louisville*, edited by J. D. Cole and E. J. Miller (University of Louisville, Kentucky) 1985, pp. 4-8.
[10] Boscaleri A. *et al.*, *Meas. Sci. Technol.*, **5** (1994) 190.
[11] Ventura G. *et al.*, TESRE / CNR Int. Rep. N. 169 (1994).
[12] Brighenti A. *et al.*, TESRE / CNR Int. Rep. N. 148 (1990).